

Symmetry, dimension and the distribution of the conductance at the mobility edge

Marc Rühländer¹, Peter Markoš^{1,2} and C. M. Soukoulis¹

¹Ames Laboratory and Department of Physics and Astronomy, Iowa State University, Ames, Iowa 50011

²Institute of Physics, Slovak Academy of Sciences, Dúbravská cesta 9, 842 28 Bratislava, Slovakia

The probability distribution of the conductance at the mobility edge, $p_c(g)$, in different universality classes and dimensions is investigated numerically for a variety of random systems. It is shown that $p_c(g)$ is universal for systems of given symmetry, dimensionality, and boundary conditions. An analytical form of $p_c(g)$ for small values of g is discussed and agreement with numerical data is observed. For $g > 1$, $\ln p_c(g)$ is proportional to $(g - 1)$ rather than $(g - 1)^2$.

PACS numbers: 71.30.+h, 71.55.Jv

Disordered systems may show a transition from metallic states to insulating ones at a mobility edge,^{1,2} which separates the two regions. The probability distribution $p(g)$ of the conductance g at the critical point of disordered systems undergoing a localization–delocalization transition is still under investigation.^{3–11} Previous studies have shown that $p(g)$ depends on the symmetry of the system,⁴ its dimensionality,⁷ the boundary conditions perpendicular to the direction of transport,^{8–10} and the amount of anisotropy.^{5,12} Yet, a complete theory explaining the form of the distribution is still missing.^{3,11} Knowing that the conductance distributions are normal and log–normal in the extended, metallic and the localized, insulating regimes respectively, and taking into account the continuous nature of the Anderson localization–delocalization transition, it seems reasonable to try to combine the two forms.

In this letter we have calculated the probability distribution of the conductance for a variety of systems of different dimension and symmetry, give an approximate expression for $p_c(g)$, compare our numerical results to some analytical approximations, and present a way of explaining the differences between theory and numerical results. We find that it is necessary to examine the distributions of the smallest Lyapunov exponents and the relationship between their respective mean values. We also show that $p_c(g)$ is independent of the particular point chosen on the critical surface in parameter space, consistent with similar findings on varying the distribution function of the disorder potential.^{13,14}

We have calculated the conductance distributions at the mobility edge of a three–dimensional (3D) system with orthogonal symmetry, a two–dimensional (2D) system with symplectic symmetry, and of several 2D systems with unitary symmetry. All these systems possess a mobility edge and are modelled after the Anderson tight–binding Hamiltonian

$$\mathcal{H} = \sum_{n,\tau} |n\tau\rangle \varepsilon_n \langle n\tau| + \sum_{n,\tau,n',\tau'} |n\tau\rangle V_{n,n'} \langle n'\tau'| \quad (1)$$

where n, n' are nearest neighbour sites in the 2D or 3D

lattice. The variables τ, τ' take on values of 1 or -1 for symplectic systems with spin–orbit interactions, where the hopping integrals $V_{n,n'}$ thus become 2×2 matrices; otherwise they are scalars and the spin “variables” have only one value.¹⁵ The site energies ε_n are always independent of τ .

In Fig. 1 we show three unitary systems with periodic boundary conditions. A magnetic field perpendicular to the direction of transport facilitates the existence of critical states at the center of each Landau subband. We investigate the dependence of $p_c(g)$ on the disorder strength W . The flux per unit area α has been kept constant at $\alpha = 1/8$. For weak disorder, considerable finite size effects have to be eliminated. Even for the system shown with 192×192 lattice sites (dashed line in Fig. 1) the distribution still has not completely converged to the form obtained for the two cases of stronger disorder, where the system size is only 64×64 lattice sites (solid lines in Fig. 1). Anisotropic systems can be rescaled to the same distribution.¹² Table I contains the averages and standard deviations of the relevant variables for these ensembles as well as for those we use in later parts of this paper.

We will discuss the transmission properties of a system in terms of its “extensive Lyapunov exponents” z_i , where e^{z_i} are the eigenvalues of $T^\dagger T$ and T is the transfer matrix in the channel representation. Then, we have for the conductance g (in units of e^2/h)¹⁶

$$g = \sum_{i=1}^N \frac{1}{\cosh^2\left(\frac{z_i}{2}\right)} \quad (2)$$

where N is the number of open channels. The distribution of the conductance should therefore be discussed in connection with that of the Lyapunov exponents. The distribution of the smallest positive Lyapunov exponent z_1 can be approximated by a Wigner distribution with $\beta = 1$, independently of the actual universality class of the system:^{16,17}

$$p(z_1) \approx \frac{\pi}{2} \frac{z_1}{\langle z_1 \rangle^2} \exp\left(-\frac{\pi}{4} \frac{z_1^2}{\langle z_1 \rangle^2}\right) \quad (3)$$

where $\langle \cdot \rangle$ denotes the ensemble average. This approximation works reasonably well, if $\langle z_1 \rangle$ is small enough, which is true in two and three dimensions, but not e.g. in four.

Approximating $g \approx g_1 \stackrel{\text{def}}{=} \cosh^{-2}(z_1/2)$, we can rewrite this distribution in terms of $\ln(g)$ as

$$p(\ln g) \approx p(\ln g_1)$$

$$\begin{aligned}
&= \int_0^\infty \delta\left(\ln(g) + 2 \ln \cosh\left(\frac{z_1}{2}\right)\right) p(z_1) dz_1 \\
&\approx \frac{\pi}{2 \langle z_1 \rangle^2} \frac{z_1}{\tanh \frac{z_1}{2}} \exp\left(-\frac{\pi}{4} \frac{z_1^2}{\langle z_1 \rangle^2}\right) \quad (4)
\end{aligned}$$

evaluated at $\ln(g) = -2 \ln \cosh(z_1/2)$. This obviously neglects contributions to the conductance from higher channels and therefore overestimates the distribution in the range $\ln(g) \leq 0$. Note, that, because $\cosh^2(z_1/2) \geq 1$ for all z_1 , $\ln(g_1) \leq 0$. One finds that $p(\ln g_1)$ is already in reasonable agreement with $p(\ln g)$ indicating that the higher channels' contributions are small, though not entirely negligible. Therefore $p(\ln g_1)$ can be used as a starting point for discussion of the correct distribution of the conductance in the range $g \leq 1$. Fig. 2 shows the numerical results for 10,000 cubic systems of orthogonal symmetry with periodic boundary conditions. It can be seen clearly from Fig. 2 that both $p(\ln g_1)$ and Eq. 4 are in very good agreement with the detailed numerical results. Also shown is the distribution $p(\ln g_2)$, where $g_2 = g_1 + \cosh^{-2}(z_2/2)$, which agrees already very well with the distribution of the total conductance. Squares of symplectic symmetry behave similarly. Also, systems with hard wall boundary conditions show the same qualitative behaviour in both 3D orthogonal systems and 2D symplectic ones. A summary of the averages and variances of z_1 and z_2 can be found in Table II.

Using a different, more elaborate approach, Muttalib and Wölfle¹¹ derived for quasi-one-dimensional, weakly disordered systems a formula for the critical probability distribution over the whole range of g , including $g > 1$. It can be written as

$$p(\ln g) = \begin{cases} \frac{1}{Z} \frac{\sqrt{z_1 \sinh z_1}}{\tanh \frac{z_1}{2}} e^{-\frac{\Gamma}{4} z_1^2} & : g \leq 1 \\ \frac{\sqrt{2}}{Z} g e^{-a(g-1)^2} & : g \geq 1 \end{cases} \quad (5)$$

where the formula for the range $g \leq 1$ again needs to be evaluated at $\ln(g) = -2 \ln \cosh(z_1/2)$. The parameter Γ can be used to fit this function to the numerical results. (a is a function of Γ .) Taking $\Gamma = \pi / \langle z_1 \rangle^2$ and noting that $\sinh(z_1) \approx z_1$ for small z_1 , the similarity of Eq. 5 and Eq. 4 is apparent. This suggests replacing z_1 in the prefactor of Eq. 3 with $\sqrt{z_1 \sinh(z_1)}$. Preliminary results show that this actually results in better agreement with data even for somewhat higher values of $\langle z_1 \rangle$. It should be noted though, that in Γ instead of the average value of z_1 , one should use the most probable one, which is smaller than the average value by a factor of about 0.8 in the case of a Wigner distribution. Despite their deriving¹¹ a distribution for the whole range of g , their formula still overestimates slightly the weight of the range $g \leq 1$ in 3D systems. However, in the 2D symplectic case, they slightly underestimate this weight. A change in the fitting parameter Γ does not remedy this discrepancy in a satisfactory manner. Fig. 3 shows numerical results together with a fit according to Eq. 5. The first panel shows the distributions for 3D orthogonal systems

with $10 \times 10 \times 10$ lattice sites. In a log-linear plot one can see that Eq. 5 increasingly overestimates $p(\ln g)$ for $\ln(g) \rightarrow -\infty$. For the 2D symplectic case shown in the second panel, a fit for $\ln(g)$ close to 0 results in a very strong underestimation far from $\ln(g) = 0$. The fit presented for both kinds of boundary conditions still gives an overall underestimation of the portion of the conductance distribution¹⁸ with $g \leq 1$.

To understand the qualitatively different behaviours of this theoretical approach, one has to look at the averages of the higher Lyapunov exponents.¹⁷ In the quasi-one-dimensional, weakly disordered case for which Eq. 5 was derived, one has $\langle z_2 \rangle = 2 \cdot \langle z_1 \rangle$, independent of dimension, symmetry or boundary conditions.^{16,17,19} For the 3D orthogonal ensemble, one finds at the critical point that $\langle z_i \rangle^2 \propto i$, and thus $\langle z_2 \rangle$ is significantly smaller than $2 \cdot \langle z_1 \rangle$,¹⁷ so that the contribution of the second channel is higher than expected from Eq. 5, whereas for the 2D symplectic case, $\langle z_2 \rangle > \langle z_1 \rangle$, so that the second channel's contribution is smaller than expected. Compare the values in Table II, which support these arguments.

We also looked at the conductance distribution in the range $g \geq 1$. In order to have a sizeable ensemble for that range, we took half a million samples for 2D symplectic systems of 40×40 lattice sites with both periodic and hard wall boundary conditions as well as for 3D orthogonal systems of $10 \times 10 \times 10$ lattice sites with periodic boundary conditions. For cubes with hard wall boundary conditions we even took ten million samples. About 20% of the symplectic samples, 6% of the 3D samples with periodic boundary conditions, and 3% of the 3D samples with hard wall boundary conditions turn out to have a conductance bigger than 1. For the latter ensemble, only about 470 out of the ten million samples have a conductance $g > 2$ and only one sample can be found with $g > 3$. We find that in the range $g > 1$, $\ln p_c(g)$ is at most linear in $(g - 1)$, as can be seen from Fig. 4. This is in disagreement with the theory presented by Muttalib and Wölfle,¹¹ which predicts a quadratic dependence with a logarithmic correction, and which therefore expects a positive first derivative of $\ln p_c(g)$ in g . Finally, Fig. 4 shows that the first derivative of $p_c(g)$ is discontinuous²² at $g = 1$. We suppose that this non-analytical behaviour was not taken into account by the analysis of Muttalib and Wölfle.¹¹

In conclusion, we have shown that the critical distribution of the conductance in disordered systems is universal for systems of given dimensionality, universality class, and boundary conditions. We show further that for systems of quite different types, the total conductance is distributed only slightly differently from the distribution of the first channel, and give arguments for the quality of corrections depending on the statistics of the second channel. We present a formula for $p_c(\ln g)$ which agrees reasonably well with the numerical results in the range $g \leq 1$. Finally, we found non-analyticity of $p_c(g)$ at $g \approx 1$ and estimated an exponent of roughly 1 in $\ln p_c(g)$ as a function of $g - 1$ rather than the predicted exponent of

2.

Ames Laboratory is operated for the U.S. Department of Energy by Iowa State University under Contract No. W-7405-Eng-82. This work was supported by the Director for Energy Research, Office of Basic Science. P.M. would like to thank Ames Laboratory for their hospitality and support and the Slovak Grant Agency for financial support.

-
- ¹ C. M. Soukoulis and E. N. Economou, *Waves in Random Media* **9**, 255 (1999) and references therein.
- ² For a recent review, see B. Kramer, and A. MacKinnon, *Rep. Prog. Phys.* **56**, 1469 (1993).
- ³ B. Shapiro, *Philos. Mag. B* **56**, 1031 (1987); A. Cohen, Y. Roth and B. Shapiro, *Phys. Rev. B* **38**, 12125 (1988); B. Shapiro, *Phys. Rev. Lett.* **65**, 1510 (1990).
- ⁴ K. Slevin and T. Ohtsuki, *Phys. Rev. Lett.* **78**, 4083 (1997).
- ⁵ X. Wang, Q. Li, and C. M. Soukoulis, *Phys. Rev. B* **58**, 3576 (1998); X. Wang, Q. Li, and C. M. Soukoulis, *Physica B* **296**, 280 (2001).
- ⁶ V. Plerou and Z. Wang, *Phys. Rev. B* **58**, 1967 (1998).
- ⁷ P. Markoš, *Phys. Rev. Lett.* **83**, 588 (1999).
- ⁸ C. M. Soukoulis, X. Wang, Q. Li, and M. M. Sigalas, *Phys. Rev. Lett.* **82**, 668 (1999).
- ⁹ K. Slevin, T. Ohtsuki, and T. Kawarabayashi, *Phys. Rev. Lett.* **84**, 3915 (2000).
- ¹⁰ D. Braun, E. Hofstetter, G. Montambaux and A. MacKinnon, *cond-mat/0101122*.
- ¹¹ K. A. Muttalib and P. Wölfle, *Phys. Rev. Lett.* **83**, 3013 (1999).
- ¹² M. Rühländer, P. Markoš, and C. M. Soukoulis, *cond-mat/0103594*.
- ¹³ P. Markoš, *Europhys. Lett.* **26**, 431 (1994).
- ¹⁴ K. Slevin and T. Ohtsuki, *Phys. Rev. B* **63**, 045108 (2001).
- ¹⁵ An external magnetic field enters the Hamiltonian via its vector potential \mathbf{A} ($\nabla \times \mathbf{A} = \mathbf{B}$), which appears in the phases of the hopping integrals: $V_{n,n'} = t_{n,n'}^0 e^{-2\pi i(e/h) \int_{\mathbf{r}_n}^{\mathbf{r}_{n'}} \mathbf{A}(\mathbf{r}) d\mathbf{r}}$. The integral connects the lattice sites n (at \mathbf{r}_n) and n' (at $\mathbf{r}_{n'}$) in a straight line. The Evangelou-Ziman model²⁰ incorporates spin-orbit coupling by using the following hopping integrals: $V_{n,n'}^{\tau,\tau'} = t_{n,n'}^0 [\delta_{\tau,\tau'} + \mu i \sum_{\nu} \sigma_{\tau,\tau'}^{\nu} t_{n,n'}^{\nu}]$ where $\nu = x, y, z$ and σ^{ν} are the Pauli matrices. The parameter μ characterizes the strength of the spin-orbit interaction. The Ando model²¹ exhibits the same conductance distributions.¹³ The hopping parameter $t_{n,n'}^0$ is chosen constant in all our systems, where disorder is introduced only by choosing the site energies ε_n independently from a rectangular distribution of width W centered at 0. Thus we have in W a measure of the disorder strength. Again, other types of distributions for ε_n are known to give the same distributions of the conductance.¹⁴ For orthogonal systems we write $V_{n,n'} = t_{n,n'}^0$ for consistency with the other models.
- ¹⁶ J.-L. Pichard, *NATO ASI Ser B* **154**, 369 (Plenum Press,

New York, 1991).

- ¹⁷ P. Markoš and B. Kramer, *Philos. Mag. B* **68**, 357 (1993); P. Markoš, *J. Phys. I (France)* **4**, 551 (1994); P. Markoš, *J. Phys. Cond. Matt.* **7**, 8361 (1995).
- ¹⁸ As mentioned earlier, the average $\langle z_1 \rangle$ does not result in a satisfying fit of Eq. 5 with $\Gamma = \pi / \langle z_1 \rangle^2$, although for 3D systems the best-fit-value is smaller than $0.8 \cdot \langle z_1 \rangle$, whereas for 2D systems it is closer to $\langle z_1 \rangle$.
- ¹⁹ O. N. Dorokhov, *JETP Lett.* **36**, 318 (1982); P. A. Mello, P. Pereyra, and N. Kumar, *Ann. Phys. (N.Y.)* **181**, 290 (1988).
- ²⁰ S. N. Evangelou and T. Ziman, *J. Phys. C* **20**, L235 (1987).
- ²¹ T. Ando, *Phys. Rev. B* **40**, 5325 (1989).
- ²² We found $\partial p_c(g) / \partial g$ of order -100 as $g \rightarrow 1^+$ in 3D systems with hard wall boundary conditions.

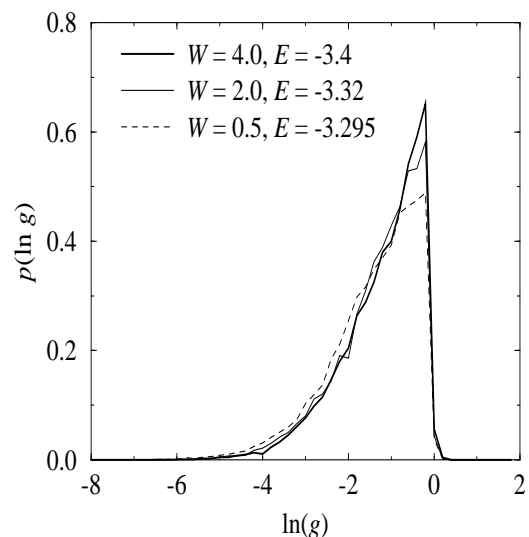


FIG. 1. The conductance distributions for three different critical two-dimensional systems with a magnetic field perpendicular to the plane.

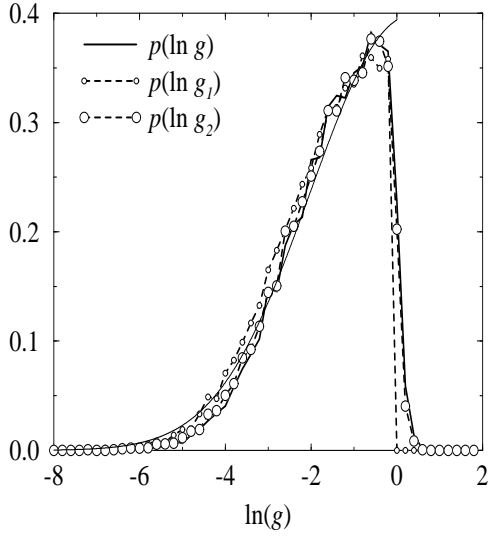


FIG. 2. The distribution of the total conductance g of cubes with $10 \times 10 \times 10$ lattice sites and periodic boundary conditions, together with the distributions for the contributions from the first (g_1) and the first two (g_2) channels of the same ensemble. The thin solid line is the result of Eq. 4 with $\langle z_1 \rangle = 2.825$.

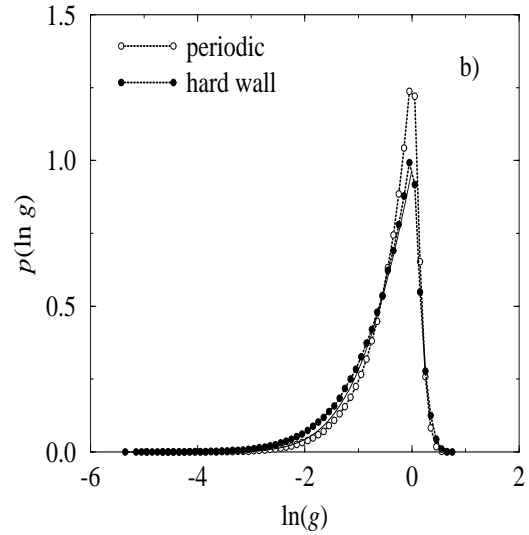
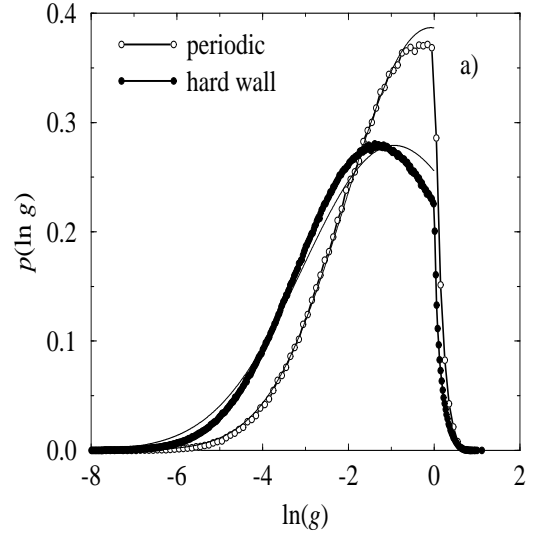


FIG. 3. The conductance distributions for a) three-dimensional systems of orthogonal symmetry with $10 \times 10 \times 10$ lattice sites and b) two-dimensional systems of symplectic symmetry with 40×40 lattice sites (thick lines). The thin lines are fits to the data according to Eq. 5 with $\Gamma = \pi/(2.2)^2$, $\Gamma = \pi/(2.55)^2$, and $\Gamma = \pi/(1.4)^2$ for the 3d periodic, 3d hard wall, and 2d cases respectively.

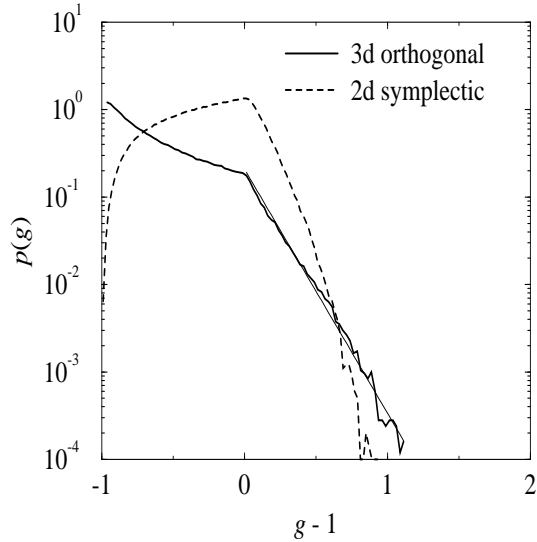


FIG. 4. The distribution for an ensemble of 500,000 cubic systems (thick line) shows a behaviour $\ln p = \text{const.} + (g-1)^\alpha$ with $\alpha \approx 1$ (thin line) in the region $g \geq 1$ and a discontinuity in its first derivative at $g = 1$. The distribution for an ensemble of 500,000 square systems behaves similarly. Both cases shown use periodic boundary conditions.

TABLE I. The averages and variances of the conductance and its logarithm for the ensembles we used in this work. O, U, S: orthogonal, unitary, symplectic; p, h: periodic, hard wall boundary conditions. Unitary systems use periodic boundary conditions. N_{stat} : number of samples.

System	N_{stat}	$\langle g \rangle$	σ_g^2	$\langle \ln(g) \rangle$	$\sigma_{\ln(g)}^2$
2d U, $W = 4$	10,000	0.445	0.082	-1.120	0.842
2d U, $W = 2$	10,000	0.428	0.079	-1.172	0.887
2d U, $W = 0.5$	10,000	0.393	0.078	-1.306	1.027
2d S, p	500,000	0.749	0.088	-0.401	0.283
2d S, h	500,000	0.691	0.108	-0.531	0.418
3d O, p	500,000	0.391	0.108	-1.418	1.282
3d O, h	10,000,000	0.284	0.087	-1.929	1.762

TABLE II. The averages and variances of the two smallest Lyapunov exponents. $N_{\text{stat}} = 10,000$.

System	$\langle z_1 \rangle$	$\sigma_{z_1}^2$	$\langle z_2 \rangle$	$\sigma_{z_2}^2$
2d S, p	1.424	0.621	3.987	0.924
2d S, h	1.635	0.811	4.065	1.186
3d O, p	2.825	1.918	4.965	1.829
3d O, h	3.411	2.475	5.518	2.132